Mantle Plumes and Entrainment: Isotopic Evidence

S. R. Hart, E. H. Hauri, L. A. Oschmann, J. A. Whitehead

Many oceanic island basalts show sublinear subparallel arrays in Sr-Nd-Pb isotopic space. The depleted upper mantle is rarely a mixing end-member of these arrays, as would be expected if mantle plumes originated at a 670-kilometer boundary layer and entrained upper mantle during ascent. Instead, the arrays are fan-shaped and appear to converge on a volume in isotopic space characterized by low $^{87}Sr/^{86}Sr$ and high $^{143}Nd/^{144}Nd$, $^{206}Pb/^{204}Pb$, and $^{3}He/^{4}He$ ratios. This new isotopic component may be the lower mantle, entrained into plumes originating from the core-mantle boundary layer.

Oceanic islands are volcanic features produced by magmas derived from partial melting of underlying mantle upwellings or plumes. The isotopic chemistry of these plumes, as sampled by the island volcanism, is quite variable and yet distinctly different from that of the mantle that is upwelling under mid-ocean spreading ridges. The chemistry of oceanic island volcanism may thus be used to "map" different regions of the mantle.

The isotopic taxonomy of oceanic basalts allows one to identify (*1*, *2*) at least four mantle components, reservoirs or "species" (*3*), which Zindler and Hart (*4*) termed DMM [depleted mid-ocean ridge basalt (MORB) mantle], HIMU (high U/Pb mantle), and EM1 and EM2 (enriched mantle 1 and 2). The origin, evolution, and present habitat of these four species is the subject of considerable debate (*5*). Original distinction of these species was based on Sr, Nd, and Pb isotopic characteristics, but additional isotopic and trace element distinctions have been cataloged (*6*–*8*). All four species appear to be "interbreedable," and the consequent isotopic mixing lines may be useful in establishing the locations and interactions of these mantle components. In this report, we address the ramifications of one particular kind of mixing: entrainment by ascending mantle plumes. We suggest that a new mantle species should be identified, probably the lower mantle.

There are some 570 oceanic basalts [OIB (oceanic island basalt) and MORB] for which combined Sr, Nd, and three Pb isotopic values are available. When plotted in Sr, Nd, and Pb isotopic space (Fig. 1), these data lie largely within a tetrahedron delineated by the four mantle end-members (DMM, HIMU, EM1, and EM2). The focusing of the data into the corners of the tetrahedron (Fig. 1) suggests that the end-members are fairly restricted in composition (particularly the MORB and HIMU end-members). Most of the data also fall close to the DMM-HIMU-EM1 base triangle of the tetrahedron (seen edge-on in Fig. 1B); this is close to the three-component mantle plane defined by Zindler *et al.* (*9*).

To pursue the question of whether four end-member mantle species are sufficient to circumscribe the oceanic isotopic data set, we have run a principal component analysis similar to work by Allègre *et al.* (*10*) on a smaller data set. The percentage of variance accounted for by the five eigenvectors is 56.6, 37.2, 3.7, 1.8, and 0.7% (*11*). Thus, the planar aspect of the data in Fig. 1 is confirmed, because the first two eigenvectors account for 93.8% of the population variance. The first three eigenvectors account for 97.5% of the variance [similar to the value of 99.2% reported by Allègre *et al.* (*10*)]. Because the data set is composed of five isotopic values for each sample, in five-dimensional isotopic space the polygon containing the fewest vertices ($n + 1$) is a simplex, and the oceanic data set could theoretically require six end-members to completely define it. Because three eigenvectors account for 97.5% of the variance, we can treat the data as a tetrahedron in three dimensions without misrepresenting any significant amount of information. The robustness of this conclusion is affirmed by adding an additional isotopic dimensionality (for example, Hf) and noting that the four end-members are still sufficient to circumscribe the data (*6*, *12*). Other isotopic systems (for example, He) do not support this premise and appear to require an end-member that is not obvious in the heavy isotope data set (*13*). We address this paradox below. For simplicity, we have chosen to use three isotopic dimensions, not the first three eigenvectors, to plot the oceanic data in Fig. 1. This is justified because the two excluded isotopic dimensions ($^{207}Pb/^{204}Pb$ and $^{208}Pb/^{204}Pb$) are highly correlated with $^{206}Pb/^{204}Pb$.

Data from many individual islands and island groups show elongated data arrays that are suggestive of mixing between various mantle reservoirs (Fig. 2). The arrays show a fairly consistent fan-shaped arrangement and are not haphazardly strewn through isotopic space. In addition, they are pseudolinear, without marked curvature. As argued by Hart *et al.* (*14*) and Hart (*5*), this linearity implies that the relative abundances of Sr, Nd, and Pb in the end-members are similar and that it is unlikely that there are major compositional differences among the end-members. Not all islands that show large isotopic variations show elongated arrays, however. For example, data plots from Iceland and Ascension (Fig. 2B) and from others not shown in Fig. 2 (Canaries, New England Seamounts, western Cook-Australs, and others) tend to be blobby or platelike in three-dimensional space. We assume that these simply represent mixtures of more than two components. The arrays are not always mixing

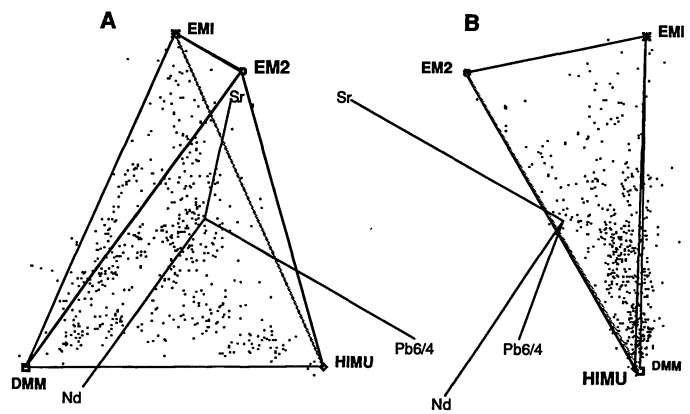

Fig. 1. Two "views" of the tetrahedron, defined by the four mantle end-members of Zindler and Hart (*4*). There are 483 OIBs and 89 N-MORBs plotted in three-dimensional isotopic space ($^{87}Sr/^{86}Sr$, $^{143}Nd/^{144}Nd$, and $^{206}Pb/^{204}Pb$); projections of these three coordinate axes are shown on both panels. (**A**) View normal to the DMM-HIMU-EM1 base triangle; the EM2 corner of the tetrahedron is above the base plane. (**B**) View, rotated 90°, directly into the DMM-HIMU-EM1 base triangle; this view shows that most of the data lie close to the base "mantle plane." DMM was chosen to have the most depleted Sr and Nd of any MORB (0.7022, 0.5133, and 18.00), EM1 was chosen to be the most enriched sample of the Walvis array (0.7053, 0.51236, and 17.40), HIMU was chosen to be like the most radiogenic Pb sample from Mangaia (0.70285, 0.51285, and 21.80), and EM2 was chosen to be similar to the most radiogenic Sr samples from Tahaa and Samoa (0.7078, 0.51258, and 19.00).

Woods Hole Oceanographic Institution, Woods Hole, MA 02543.

between the hypothesized pure mantle species; many originate (terminate?) from binary joins of the tetrahedron (for example, the Cameroon line: HIMU-EM1; Azores: HIMU-EM2; and Kerguelen and Tristan: EM1-EM2).

The DMM end-member is rarely a parent to any of these arrays; that is, of the many arrays shown in Fig. 2, none are headed toward the DMM apex itself. This has been pointed out before for individual cases such as Walvis ridge (*15*) and Heard Island (*16*). The Hawaiian array appears headed toward average N-MORB (MORB sample from normal-depth ridges); however, this is largely a result of the projection used for Fig. 2. When viewed from the edge (Fig. 3), the Hawaiian array is rising out of the DMM-HIMU-EM1 base plane such that its extension only marginally intersects any of the N-MORB field. New data for the Galápagos (*17*) do define an elongate array that trends directly into the N-MORB field. Wherever the HIMU and EM reservoirs are thought to reside in the mantle, they must either rise through, or circulate in, the upper DMM mantle. Of all of the possible mantle mixing scenarios, the DMM reservoir is the most obvious candidate to be a common component in any mixture. Only basalts from Iceland and the Galápagos Islands appear to extend into the N-MORB field. Ridge-centered hot spots such as these might be expected to be most susceptible to incorporation of a DMM component. Of the other islands that show elongate arrays, DMM is virtually absent as an identifiable component. Although there is a striking fan-shaped pattern to the OIB arrays in Fig. 2, the convergence or focal area is not well defined and contains few data. The characteristics of the missing parent species for this focal zone are depleted Sr and Nd ratios (probably <0.7025 and >0.5131) accompanied by high $^{206}Pb/^{204}Pb$ (19.1 to 19.7).

Several possible models are suggested by the above observations:

1) The upper MORB mantle contains HIMU components dispersed within it that are sampled preferentially by transiting plumes or diapirs relative to the mixture that is sampled by melting on ridges. For example, the upper mantle may be DMM with <10% HIMU dispersed within it as discrete reservoirs. Representative sampling on ridges gives the N-MORB field as shown; mixing of this two-component upper mantle with transiting diapirs and plumes, followed by melting that preferentially samples the HIMU component, could give mixing arrays that appear to have an end-member midway along the HIMU-DMM join.

2) There is an actual parent (mantle reservoir) with isotopic characteristics representative of the focal zone, but this parent is rarely or never sampled in pure form. We term this new species FOZO (Focus Zone). If FOZO is not in the upper mantle (Model 1), it must lie beneath the upper mantle, either in a boundary layer at 670 km (670 BL), at the core-mantle boundary (CMBL), or in the lower mantle. Several mixing scenarios are then possible: (i) plumes containing EMs and HIMU components from the lower mantle (or the CMBL) (*18*) entrain FOZO materials from the 670 BL; (ii) plumes containing EMs and HIMU components from the CMBL entrain FOZO from the lower mantle, and no components are derived from the 670 BL; or (iii) FOZO plumes from the CMBL or lower mantle entrain EMs and HIMU components from

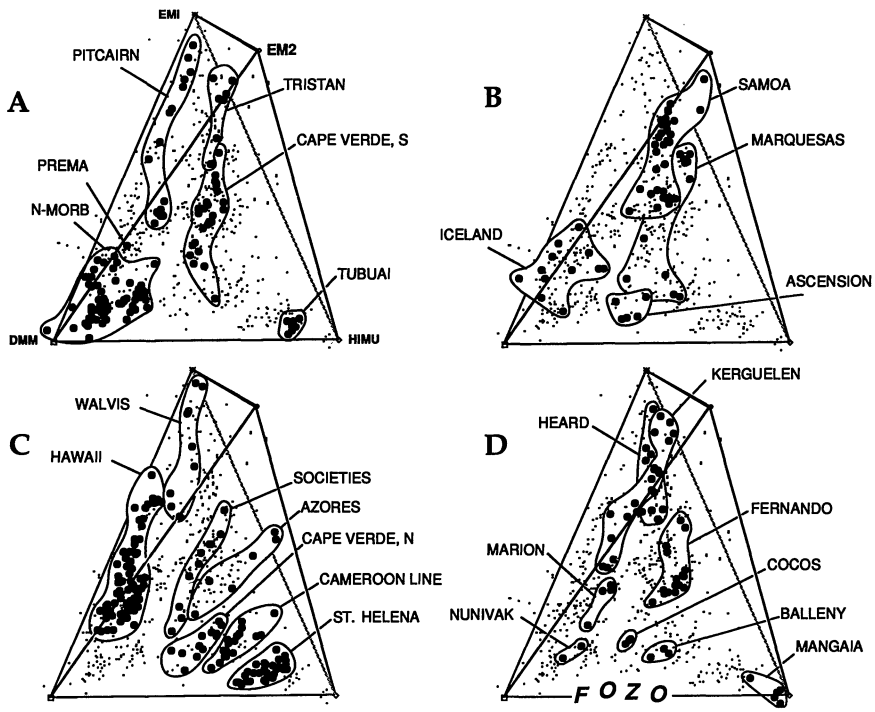

Fig. 2. Projection of various oceanic isotopic data sets onto base triangle of mantle tetrahedron; same view as in Fig. 1A. All available data that show any semblance of "elongated" arrays are plotted (large points), excluding only those arrays based on fewer than four samples. There are a number of data sets not shown, involving significant numbers of samples, that are not obviously "elongate" (for example, Canaries, New England Seamounts, and Raratonga). We have also shown a few data sets for general interest that are either not elongate (Iceland and Ascension) or that contain limited numbers of samples (Cocos, Nunivak, and Balleny). The PREMA component of Zindler and Hart (*4*) is also shown for reference. The data sets are limited to basaltic rocks, and in the case of the N-MORB, most data are for glasses. N-MORBs are defined as MORB samples from normal-depth ridges with $^{87}Sr/^{86}Sr < 0.7030$ (72 out of 89). N-MORB with anomalously high $^{206}Pb/^{204}Pb$ ratios have been reported from the Easter microplate (*40*); although no Nd data are reported, these samples will undoubtedly plot in the FOZO area. Cape Verde has been divided into two geographic groups on the basis of the discussion in Gerlach *et al.* (*41*); the Cameroon line data (*42*) are limited to basalts from the oceanic sector, and Pagalu has been omitted because it lies well away from the general trend. The tendency for most of the island fields to converge toward the bottom of the base triangle is clear; they are not converging toward typical N-MORB. For orientation, the F of the word FOZO [in (**D**)] would have approximate isotopic values of 0.7025, 0.51318, and 19.07; values for the Z would be 0.70248, 0.51310, and 19.65. Data sources are as summarized in Hart (*5*) and in (*16, 43*).

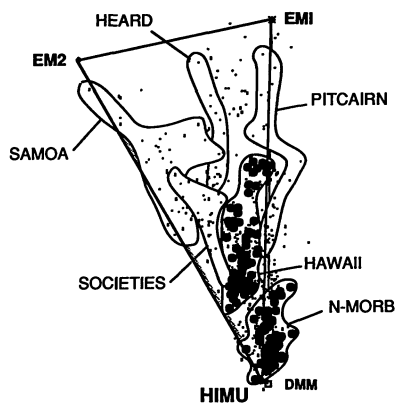

Fig. 3. "Side" view (as in Fig. 1B), showing the Hawaiian and N-MORB fields (and several others for comparison). The Hawaiian array does not appear to be mixing toward N-MORB, but instead is apparently aiming to the left of the general N-MORB field. The N-MORB field scatters around the DMM-EM1-HIMU base triangle, suggesting possible contamination of DMM with EM1 and HIMU, but not with EM2.

the lower mantle or 670 BL. No significant upper mantle DMM entrainment would take place in Model 2.

Because compelling evidence for layered versus whole-mantle convection is still elusive (*19*), no definitive choices are possible among these scenarios. Arguments have been made that EM- or HIMU-rich reservoirs are located in the deep mantle on the basis of their prominence in the DUPAL (*20*) anomaly and the correlation of the DUPAL anomaly with low-degree features of the geoid (*21*) and with lower mantle–CMBL seismic velocity anomalies (*5, 11, 22, 23*). If this location is correct (that is, if EMs and HIMU components are concentrated in the CMBL), then the FOZO reservoir would be either the lower mantle itself or the 670 BL. If it is the 670 BL, then we need to explain why plumes originating from the CMBL entrain material from the 670 BL but not material from the lower and upper mantles. We address this selective entrainment problem in more detail below.

The He isotope data are not obviously consistent with the four mantle end-members as defined from Sr, Nd, Pb, and Hf. We believe the FOZO reservoir defined above may also be the high-^{3}He component, which has not heretofore been identified with the heavy isotope end-members. For example, samples in the upper end of the Hawaiian array (Fig. 2C, Koolau and Lanai) have ^{3}He/^{4}He ratios of 10 to 16 Ra (*24–26*), whereas samples from the lower end (Loihi) have ratios of 20 to 35 Ra (*13*). Samples from São Miguel (Fig. 2C, Azores) have low ratios (3.5 Ra) at the upper end that increase to 8.5 Ra at the lower end (*27*). The ^{3}He/^{4}He ratios increase from 8 to 25 Ra (*28*) moving downward along the Samoa array (Fig. 2B). Helium data are not available for samples defining the other arrays of Fig. 2, but the other known islands with high ^{3}He/^{4}He [Réunion, Carolines, Iceland, Galápagos, Juan Fernandez, Erebus, and Bouvet (*29, 30*)] all tend to lie below the middle of the tetrahedron (Fig. 2). In contrast, many of the low-^{3}He/^{4}He islands tend to be rich in EM [Samoa, Azores, Tristan, and Kerguelen (*13, 27, 28, 30*)] or HIMU [St. Helena and Tubuai (*31*)] components. This identity of FOZO and the high ^{3}He/^{4}He ratios are also consistent with the observation that the MORB source, which appears to have consistent ^{3}He/^{4}He ratios of ~8.5 Ra, does not seem to be a mixing end-member for any of the arrays in Fig. 2, either for heavy isotopes or for He. This hypothesis can be tested by more detailed studies involving both He and Sr, Nd, and Pb on basalts from key islands such as Iceland, Galápagos, Juan Fernandez, Cape Verde, and the Cameroon line.

If FOZO does indeed have a high ^{3}He/^{4}He ratio, then the model discussed above, in which FOZO is an upper mantle mixture of DMM and HIMU, clearly fails, because neither DMM nor HIMU is characterized by high ^{3}He/^{4}He ratios (~8.5 Ra for DMM and 5 to 7 Ra for HIMU). On the other hand, any of the three Model 2 scenarios involving FOZO in the 670 BL, CMBL, or lower mantle would be acceptable, although perhaps not equally plausible. The choice would be connected with the mechanism for producing high ^{3}He/^{4}He in FOZO. High ^{3}He/^{4}He ratios are typically ascribed to mantle that is more primitive, whereas the Sr and Nd isotopic character of FOZO mantle clearly is not primitive but rather depleted. FOZO could be formed by extracting U and Th relative to He to leave a depleted residual mantle with high He/U and He/Th. Extant partitioning data (*32*) suggest that U and Th are more incompatible than is He. If FOZO was depleted early in the earth's history relative to DMM, then it could retain a higher ^{3}He/^{4}He ratio than DMM. Alternatively, if FOZO is the CMBL or lowermost mantle, it may be replenished with primordial He from the core.

A further constraint on the nature of the FOZO species may be derived from consideration of the thermal entrainment process, whereby heat flows from a plume, adding to the buoyancy and lowering the viscosity of the surrounding mantle. This material rises then both by simple buoyancy and by viscous coupling to the plume. There may or may not be any extensive mixing in this process before melting, depending on whether material is entrained into a diapir or plume head (*33*), a tilted plume conduit (*34*), or an established vertical conduit (*35*).

The amount of entrainment (that is, the mass of new surrounding mantle added to an initial mass of transiting plume) will increase as the plume ascends. We assume that entrainment is a significant phenomenon, although certain models and choices of mantle properties may lead to the conclusion that entrainment is insignificant (*36*). We are particularly interested in the relative masses of upper mantle versus lower mantle entrained into plumes or diapirs originating from the CMBL. For a vertical steady-state conduit, the entrained mass flux is directly proportional to height in the conduit for both Newtonian (*37*) and power law rheologies (*35*), so the entrained upper mantle mass flux simply constitutes 670 km/2900 km, or 23%, of the total entrained mass flux. At the other extreme, for an isolated spherical diapir, the entrained mass is proportional to the cube of the normalized height (*33*). Depending on the values chosen for the various material properties, the entrained upper mantle mass may constitute some 45 to 55% of the total entrained mass (that is, the upper mantle is overrepresented in the material reaching the surface).

Other cases are intermediate; a spherical diapir fed by a conduit entrains mass as height to the power of 9/5 (*38*), and a tilted conduit entrains mass flux as a normalized height to the power of 4/3 (*34*). These relations are for cases where the plume and ambient mantle are compositionally identical (no chemical buoyancy) and predict that a plume originating from the CMBL will proportion its entrained mass (or mass flux) at about 45 to 75% from the lower mantle (below 670 km) and 25 to 55% from the upper mantle (above 670 km); some 7% could represent 670 BL if that boundary layer is 200 km thick. Overrepresentation of any depth zones in the entrained fraction could arise if the particular material was not compositionally the same as the plume and thus had either lower intrinsic density or a more temperature-dependent viscosity function.

The lack of an upper mantle (DMM) signature in the mixing arrays of Fig. 2 may thus reflect the fact that only one-fourth of the entrained mantle would be DMM (versus three-fourths from the lower mantle if FOZO is lower mantle). Underrepresentation of entrained DMM could also result from its lower temperature relative to material entrained earlier (deeper); smaller amounts of melt would be generated in the entrained DMM than in the higher temperature materials. It seems unlikely, then, that FOZO resides in the 670 BL (if only 200 km thick) because it would have to be strongly overentrained relative to DMM to swamp the DMM signature. Thus, Models 2ii or 2iii are most easily reconciled with the ^{3}He/^{4}He data, the correlations of the DUPAL anomaly with both the geoid and lower mantle tomography, and the predictions from entrainment theory. Important tests of this FOZO model can be provided by combined He-Sr-Pb-Nd analyses of oceanic basalts from key islands, such as Ascension, Iceland, Galapagos, the Cameroon line, and Cape Verde.

REFERENCES AND NOTES

1. W. M. White, *Geology* **13**, 115 (1985).
2. C. J. Allègre and D. L. Turcotte, *Geophys. Res. Lett.* **12**, 207 (1985).
3. A. W. Hofmann, *Caltech Plume Symposium Abstract Volume* (Plumacy, Pasadena, CA, 1991), pp. 165–168.
4. A. Zindler and S. R. Hart, *Annu. Rev. Earth Planet. Sci.* **14**, 493 (1986).
5. S. R. Hart, *Earth Planet. Sci. Lett.* **90**, 273 (1988).
6. V. J. M. Salters and S. R. Hart, *ibid.* **104**, 364 (1991).
7. A. W. Hofmann, *Eos* **72**, 279 (1991).
8. B. L. Weaver, *Earth Planet. Sci. Lett.* **104**, 381 (1991); *Geology* **19**, 123 (1991).
9. A. Zindler, E. Jagoutz, S. Goldstein, *Nature* **298**, 519 (1982).

10. C. J. Allègre, B. Hamelin, A. Provost, B. Dupré, *Earth Planet. Sci. Lett.* **81**, 319 (1987).
11. L. A. Oschmann, thesis, Woods Hole Oceanographic Institution and Massachusetts Institute of Technology (1991).
12. P. J. Patchett, *Lithos* **16**, 47 (1983); *Geochim. Cosmochim. Acta* **47**, 81 (1983); _____and M. Tatsumoto, *Geophys. Res. Lett.* **7**, 1077 (1980).
13. M. D. Kurz, W. J. Jenkins, S. R. Hart, *Nature* **297**, 43 (1982); _____, D. Clague, *Earth Planet. Sci. Lett.* **66**, 388 (1983).
14. S. R. Hart, D. C. Gerlach, W. M. White, *Geochim. Cosmochim. Acta* **50**, 1551 (1986).
15. S. H. Richardson, A. J. Erlank, A. R. Duncan, D. L. Reid, *Earth Planet. Sci. Lett.* **59**, 327 (1982).
16. J. Barling and S. L. Goldstein, *Nature* **348**, 59 (1990).
17. W. M. White, A. R. McBirney, R. A. Duncan, in preparation.
18. A. W. Hofmann and W. M. White, *Earth Planet. Sci. Lett.* **57**, 421 (1982).
19. S. R. Hart and A. Zindler, in *Mantle Convection*, W. R. Peltier, Ed. (Gordon Breach, New York, 1989), chap. 5.
20. The DUPAL anomaly is a globe-encircling belt between the equator and 50°S in which OIB are isotopically characterized by high proportions of the EM1, EM2, and HIMU mantle components (*5, 21*).
21. S. R. Hart, *Nature* **309**, 753 (1984).
22. A. P. W. Hodder, *Tectonophysics* **134**, 263 (1987).
23. P. Castillo, *Nature* **336**, 667 (1988).
24. The unit Ra is the $^3He/^4He$ ratio in the atmosphere; thus, a basalt with 10 Ra has a $^3He/^4He$ ratio ten times that of atmospheric He.
25. B. E. Faggart, Jr., A. R. Basu, M. Tatsumoto, H. Craig, *Eos* **71**, 1669 (1990).
26. T. Trull *et al.*, *ibid.*, p. 657.
27. M. D. Kurz, R. B. Moore, D. P. Kammer, A. Gulessarian, *Earth Planet. Sci. Lett.*, in press.
28. K. A. Farley, J. Natland, J. D. Macdougall, H. Craig, *Eos* **71**, 1669 (1990).
29. M. Condomines *et al.*, *Earth Planet. Sci. Lett.* **66**, 125 (1983); K. A. Farley and H. Craig, *Eos* **70**, 1385 (1989); D. W. Graham, J. Lupton, F. Albarède, M. Condomines, *Nature* **347**, 545 (1990); M. D. Kurz, A. P. le Roex, H. J. B. Dick, *Geochim. Cosmochim. Acta*, in press; M. D. Kurz, P. S. Meyer, H. Sigurdsson, *Earth Planet. Sci. Lett.* **74**, 291 (1985); T. Staudacher, P. Sarda, C. J. Allègre, *Chem. Geol.* **89**, 1 (1990).
30. H. Craig, *Eos* **71**, 1669 (1990).
31. D. W. Graham, S. E. Humphris, W. J. Jenkins, M. D. Kurz, *Earth Planet. Sci. Lett.*, in press.
32. H. Hiyagon and M. Ozima, *Geochim. Cosmochim. Acta* **50**, 2045 (1986).
33. R. W. Griffiths, *J. Fluid Mech.* **166**, 139 (1986); *Phys. Earth Planet. Int.* **43**, 261 (1986).
34. _____ and I. H. Campbell, *Earth Planet. Sci. Lett.* **103**, 214 (1991).
35. S. R. Hart, E. H. Hauri, J. A. Whitehead, *Eos* **72**, 480 (1991).
36. D. S. Loper and F. D. Stacey, *Phys. Earth Planet. Int.* **33**, 304 (1983).
37. M. Liu and C. G. Chase, *Geophys. J. Int.* **104**, 433 (1991).
38. R. W. Griffiths and I. H. Campbell, *Earth Planet. Sci. Lett.* **99**, 66 (1990).
39. S. R. Hart, *Caltech Plume Symposium Abstract Volume* (Plumacy, Pasadena, CA, 1991), pp. 161–164.
40. D. Fontignie and J.-G. Schilling, *Chem. Geol.* **89**, 209 (1991); B. B. Hanan and J.-G. Schilling, *J. Geophys. Res.* **94**, 7432 (1989).
41. D. C. Gerlach, R. A. Cliff, G. R. Davies, M. Norry, N. Hodgson, *Geochim. Cosmochim. Acta* **52**, 2979 (1988).
42. A. N. Halliday *et al.*, *Nature* **347**, 523 (1990); A. N. Halliday, A. P. Dickin, A. E. Fallick, J. G. Fitton, *J. Petrol.* **29**, 181 (1988).
43. P. Castillo *et al.*, *Geol. Soc. Am. Bull.* **100**, 1400 (1988); D. J. Chaffey, R. A. Cliff, B. M. Wilson, in *Magmatism in the Ocean Basins*, A. D. Saunders and M. J. Norry, Eds. (Geological Society Special Publication 42, Blackwell Scientific, London, 1989), pp. 257–276; Q. Cheng *et al.*, in *Seamounts, Islands and Atolls*, B. H. Keating, P. Fryer, R. Batiza, G. W. Boehlert, Eds. (Geophysical Monograph 43, American Geophysical Union, Washington, DC, 1988), pp. 283–296; B. L. Cousens, F. J. Spera, G. R. Tilton, *Earth Planet. Sci. Lett.* **96**, 319 (1990); G. R. Davies, M. J. Norry, D. C. Gerlach, R. A. Cliff, in *Magmatism in the Ocean Basins*, A. D. Saunders and M. J. Norry, Eds. (Geological Society Special Publication 42, Blackwell Scientific, London, 1989), pp. 231–256; C. W. Devey *et al.*, *J. Geophys. Res.* **95**, 5049 (1990); C. Dupuy, H. P. Vidal, H. G. Barsczus, C. Chauvel, *Earth Planet. Sci. Lett.* **82**, 145 (1987); T. R. Elliott, C. J. Hawkesworth, K. Grönvold, *Nature* **351**, 201 (1991); I. Gautier *et al.*, *Earth Planet. Sci. Lett.* **100**, 59 (1990); D. C. Gerlach, J. C. Stormer, Jr., P. A. Mueller, *ibid.* **85**, 129 (1987); K. A. Hoernle and G. R. Tilton, *Schweiz. Mineral. Petrogr. Mitt.* **71**, 3 (1991); E. Ito, W. M. White, C. Gopel, *Chem. Geol.* **62**, 157 (1987); E. M. Klein, C. H. Langmuir, A. Zindler, H. Staudigel, B. Hamelin, *Nature* **333**, 632 (1988); A. P. le Roex, R. A. Cliff, B. J. I. Adair, *J. Petrol.* **31**, 779 (1990); Y. Nakamura and M. Tatsumoto, *Geochim. Cosmochim. Acta* **52**, 2909 (1988); H. E. Newsom, W. M. White, K. P. Jochum, A. W. Hofmann, *Earth Planet. Sci. Lett.* **80**, 299 (1986); M. Storey *et al.*, *Nature* **336**, 371 (1988); D. Weis, J. F. Beaux, I. Gautier, A. Giret, P. Vidal, in *Crust/Mantle Recycling at Convergence Zones*, S. R. Hart and L. Gulen, Eds., vol. 258 of *NATO Advanced Study Institute Series*, series C, Mathematical and Physical Science (Kluwer Academic, Norwell, MA, 1989), pp. 59–63; W. M. White, A. W. Hofmann, H. Puchlet, *J. Geophys. Res.* **92**, 4881 (1987); W. M. White *et al.*, *Eos* **70**, 1385 (1989); J. D. Woodhead and M. T. McCulloch, *Earth Planet. Sci. Lett.* **94**, 257 (1989).
44. This work was supported by NSF grant EAR 9096194 and a Mellon Initiative award from Woods Hole Oceanographic Institution. We appreciate the stimulation offered by the Keck Geodynamics Seminar, the viewpoints and arguments offered by A. Zindler, A. Hofmann, W. White, J. Blusztajn, P. Olson, and N. Shimizu, and the opportunity afforded to us by D. Anderson to present this at the Caltech Plume symposium in May 1991 (*39*). W. White kindly made his unpublished Galapagos data available to us.

29 October 1991; accepted 4 March 1992

Polyhydroxybutyrate, a Biodegradable Thermoplastic, Produced in Transgenic Plants

Yves Poirier, Douglas E. Dennis, Karen Klomparens, Chris Somerville*

Polyhydroxybutyrate (PHB), a high molecular weight polyester, is accumulated as a storage carbon in many species of bacteria and is a biodegradable thermoplastic. To produce PHB by genetic engineering in plants, genes from the bacterium *Alcaligenes eutrophus* that encoded the two enzymes required to convert acetoacetyl–coenzyme A to PHB were placed under transcriptional control of the cauliflower mosaic virus 35S promoter and introduced into *Arabidopsis thaliana*. Transgenic plant lines that contained both genes accumulated PHB as electron-lucent granules in the cytoplasm, nucleus, and vacuole; the size and appearance of these granules were similar to the PHB granules that accumulate in bacteria.

Poly-D-(−)-3-hydroxybutyrate (PHB) is an aliphatic polyester that is accumulated by many species of bacteria as storage material (*1*). Both PHB and related polyhydroxyalkanoates (PHA) are renewable sources of biodegradable thermoplastic materials (*2*). The cost of PHB produced by bacterial fermentation is substantially higher than that of other biomaterials, such as starch or lipids, that accumulate in many species of higher plants. Therefore, we investigated the feasibility of transferring the capability for PHB synthesis from bacteria to higher plants.

Y. Poirier, Department of Energy–Plant Research Laboratory, Michigan State University, East Lansing, MI 48824.
D. E. Dennis, Department of Biology, James Madison University, Harrisonburg, VA 22807.
K. Klomparens, Department of Botany and Plant Pathology and Center for Electron Optics, Pesticide Research Center, Michigan State University, East Lansing, MI 48824.
C. Somerville, Department of Energy–Plant Research Laboratory and Department of Botany and Plant Pathology, Michigan State University, East Lansing, MI 48824.
*To whom correspondence should be addressed.

In the bacterium *Alcaligenes eutrophus*, PHB is derived from acetyl–coenzyme A (CoA) by a sequence of three enzymatic reactions (*3*). The first enzyme of the pathway, 3-ketothiolase (acetyl-CoA acetyl transferase; E.C. 2.3.1.9), catalyzes the reversible condensation of two acetyl-CoA moieties to form acetoacetyl-CoA. Acetoacetyl-CoA reductase (hydroxybutyryl-CoA dehydrogenase; E.C. 1.1.1.36) subsequently reduces acetoacetyl-CoA to D-(−)-3-hydroxybutyryl-CoA, which is then polymerized by the action of PHB synthase to form PHB. The genes encoding the three enzymes involved in PHB synthesis in *A. eutrophus* have been cloned, and expression of the genes in *Escherichia coli* is sufficient for PHB production (*4–7*). Of the three enzymes involved in PHB synthesis in *A. eutrophus*, only the 3-ketothiolase is also found in the cytoplasm of higher plants, where it is involved in the synthesis of mevalonate, the precursor to isoprenoids.

Genes that encoded acetoacetyl-CoA reductase (*phbB*) and PHB synthase (*phbC*) were introduced into *Arabidopsis thaliana*